



# Investigating the effects of multiple exposure measures to traffic-related air pollution on the risk of breast and prostate cancer

Maryam Shekarzifard<sup>a</sup>, Marie-France Valois<sup>b</sup>, Scott Weichenthal<sup>b</sup>, Mark S. Goldberg<sup>b</sup>, Masoud Fallah-Shorshani<sup>a</sup>, Laure Deville Cavellin<sup>c</sup>, Dan Crouse<sup>d</sup>, Marie-Elise Parent<sup>e</sup>, Marianne Hatzopoulou<sup>a,\*</sup>

<sup>a</sup> Department of Civil and Mineral Engineering, University of Toronto, Toronto, Canada

<sup>b</sup> Division of Epidemiology, Biostatistics and Occupational Health, Faculty of Medicine, McGill University, Montreal, Canada

<sup>c</sup> Department of Civil Engineering and Applied Mechanics, McGill University, Montreal, Canada

<sup>d</sup> Department of Sociology and New Brunswick Institute for Research, Data, and Training, University of New Brunswick, Canada

<sup>e</sup> INRS–Institut Armand-Frappier Research Centre, Laval, Quebec, Canada

## ARTICLE INFO

### Keywords:

Land-use regression  
Atmospheric dispersion  
Nitrogen dioxide (NO<sub>2</sub>)  
Traffic-related air pollution  
Breast cancer  
Prostate cancer

## ABSTRACT

Traffic-related nitrogen dioxide (NO<sub>2</sub>) has been traditionally estimated using surfaces generated through land-use regression (LUR). Recently, air pollution dispersion has been used to derive NO<sub>2</sub> exposures in urban areas. There is evidence that data collection protocols and modelling assumptions can have a large effect on the resulting NO<sub>2</sub> spatial distribution. This study investigates the effects of various NO<sub>2</sub> surfaces on the risk estimates of postmenopausal breast cancer (BC) and prostate cancer (PC), both of which have already been associated with traffic-related air pollution. We derived exposures for individuals in two case control studies in Montreal, Canada using four different surfaces for NO<sub>2</sub>. Two of the surfaces were developed using LUR but employed different data collection protocols (LUR-1 and LUR-2), and the other two surfaces were generated using dispersion modelling; one with a regional model (dispersion-1) and another with a street canyon model (dispersion-2). Also, we estimated separate odds ratios (ORs) using concentrations of NO<sub>2</sub> as measures of exposure for both cancers. While the range of NO<sub>2</sub> concentrations from dispersion (4–26 ppb) was lower than the range from LUR (4–36 ppb), the four surfaces were found to be moderately correlated, with Spearman correlation coefficients ranging from 0.76 to 0.88. The ORs for BC were estimated to be 1.26, 1.10, 1.07, and 1.05 based on LUR-1, LUR-2, dispersion-1, and dispersion-2. In contrast, the ORs for PC were estimated to be 1.39, 1.30, 1.13, and 1.04 based on LUR-1, LUR-2, dispersion-1, and dispersion-2. The four exposure measures indicated positive associations but we observed higher mean ORs based on the LUR surfaces albeit with overlapping CIs. Since LUR models capture all sources of NO<sub>2</sub> and dispersion models only capture traffic emissions, it is possible that this difference is due to the fact that non-road sources also contribute to the spatial distribution in NO<sub>2</sub> concentrations.

## 1. Introduction

In urban areas, emissions from traffic constitute the main air pollution source. A wide range of studies have linked exposure to

\* Correspondence to: 35 St George Street, Toronto, ON, Canada, M5S 1A4.

E-mail address: [marianne.hatzopoulou@utoronto.ca](mailto:marianne.hatzopoulou@utoronto.ca) (M. Hatzopoulou).

traffic-related air pollution with increased incidence of asthma (Carlsten et al. 2010; Gehring et al. 2010; Snowden et al. 2014), ischemic heart disease (Gan et al. 2011; Nyhan et al. 2014; Weichenthal et al. 2011), neurodegenerative diseases (Levesque et al. 2011; Wang et al. 2009), and various forms of cancer such as breast cancer (Crouse et al. 2010), prostate cancer (Parent et al. 2013), and lung cancer (Hamra et al. 2015). In particular, exposure to nitrogen dioxide (NO<sub>2</sub>), an accepted marker of traffic-related air pollution, has been associated with various health outcomes. For example, Chen et al. (2013) showed that a 5 ppb increase in NO<sub>2</sub> exposure was associated with a 12% increase in the risk of mortality from cardiovascular disease. In a lung cancer study, Hamra et al. (2015) estimated that a 10 µg/m<sup>3</sup> increase in exposure to NO<sub>2</sub> was associated with a 4% increase in the risk of lung cancer. In another study of chronic obstructive pulmonary disease (COPD) conducted among 52,799 participants, the authors estimated that an increase in the 35-year mean NO<sub>2</sub> level by 5.8 µg/m<sup>3</sup> was associated with an increased risk of COPD by 8% (Andersen et al., 2011).

Traditionally, NO<sub>2</sub> exposure surfaces have been developed using land-use regression (LUR) models, whereby integrated NO<sub>2</sub> measurements were conducted with passive samplers. Then, exposures were modelled at the home location of study participants (Abernethy et al. 2013; Beelen et al. 2013; Dons et al. 2014; Hoek et al. 2008; Lee et al. 2014; Shekarzifard et al. 2015). With advances in air pollution instrumentation and improved knowledge of travel and activity patterns of individuals in urban areas, new methods of deriving exposure have become possible. For example, the development of NO<sub>2</sub> sensors has enabled the implementation of short-term monitoring campaigns (Austin et al. 2006; Deville Cavellin et al. 2016; Setton et al. 2011) and personal measurements (Mcadam et al., 2011; Pattinson et al. 2014) while improvements in travel demand forecasting and traffic modelling motivated the development of traffic emission and dispersion models, capable of capturing the spatio-temporal variability in air pollution within urban areas (Beckx et al. 2009; Hatzopoulou and Miller 2010; Shekarzifard et al. 2017). LUR modelling necessitates the deployment of large air quality sampling campaigns with extensive spatial and temporal coverage (Beelen et al. 2013; Lee et al. 2014; Levy et al. 2010).

As an alternative to statistical techniques, dispersion modelling involves constructing a dynamic model of the dispersion processes occurring at the intra-urban scale. In this context, dispersion models capable of simulating air quality at the level of individual roads are grouped into 3 main categories: 1) Gaussian dispersion models, which are typically used for areas without obstacles or with obstacles of simple geometry; these models can be accurate at the top of the urban canopy and are mainly Gaussian plume and Gaussian puff models (Cimorelli et al. 2005; Scire et al. 2000); 2) Street-canyon models, which are appropriate for cities with tall buildings; they simulate pollutant transfer along the street and at intersections (Hertel and Berkowicz 1989; Soulhac et al. 2011); and 3) Computational Fluid Dynamics (CFD) models; they provide detailed representations of the atmospheric flow and some also treat the physics and chemistry of air pollutant transformations; they are however limited to local applications such as the impact of a single pollution source in complex street geometry and flow characteristics (Eichhorn and Kniffka 2010; Milliez and Carissimo 2007). Dispersion modelling of road traffic sources has been conducted for a variety of road and network configurations (Batterman et al. 2010; Hatzopoulou and Miller 2010; Lee et al. 2009; Ning et al. 2005; Sangkapichai et al. 2010). Output from dispersion models has been used in previous epidemiologic studies (Bellander et al. 2001; Gauderman et al., (2005); Henderson. et al., 2011; Nafstad et al. 2003; Raaschou-Nielsen et al. 2010). For example, in a 27-year follow-up study, Nafstad et al. (2003) estimated NO<sub>2</sub> concentrations using sets of dispersion field coefficients given from model calculations for each year. The authors estimated 8% increase in the risk of lung cancer (95% CI: 1.02–1.15) for a 10 µg/m<sup>3</sup> increase in NO<sub>2</sub> at the home address. Gauderman et al., (2005) used the CALINE4 dispersion model to estimate traffic-related NO<sub>x</sub> and estimated that with an increase in NO<sub>2</sub> concentrations by 5.7 ppb, the odds ratio (OR) for childhood asthma was 1.83 (95% CI: 1.04–3.21). Raaschou-Nielsen et al. (2010) used the OSPM dispersion model to estimate traffic related NO<sub>x</sub> concentrations and estimated that the incidence rate ratios for lung cancer were 1.30 (95% CI: 1.07–1.57) and 1.45 (95% CI: 1.12–1.88) for NO<sub>x</sub> concentrations of 30–72 µg/m<sup>3</sup> and greater than 72 µg/m<sup>3</sup>, respectively. Furthermore, in a case-control study of stillbirths, Ithrig et al. (1998) estimated arsenic exposure levels from airborne emissions using a dust dispersion model in Texas and the OR observed for Hispanics in the high exposure group (> 100 µg/m<sup>3</sup> arsenic) was 8.4. Henderson. et al., (2011) estimated smoke-related PM<sub>10</sub> from the CALPUFF dispersion model and estimated the ORs for a 30 µg/m<sup>3</sup> increase in tapered element oscillating microbalance (TEOM)-based PM<sub>10</sub> to be equal to 1.05 (95% CI: 1.03–1.06) for all respiratory physician visits, 1.16 (95% CI: 1.09–1.23) for asthma-specific visits, and 1.15 (95% CI: 1.00–1.29) for respiratory hospital admissions. Finally, Bellander et al. (2001) estimated NO<sub>2</sub> concentrations using the AIRVIRO dispersion model for all years spanning between 1955 and 1990 for the entire Stockholm area and assigned the NO<sub>2</sub> exposures to 10,800 geocoded addresses. They concluded that while this technique has practical applications for epidemiological studies, it might be limited to study sites that possessed historical traffic and other emission data.

The main strength of LUR is the use of monitoring data and the relative ease of model development. Dispersion models have the advantage of incorporating both spatial and temporal variation of air pollution within a study area and can be applied at different spatial scales. Some of the limitations of these models include the assumptions about dispersion patterns (e.g., Gaussian dispersion), the need for validation against monitoring stations, and relatively costly meteorological and emission data inputs (Jerrett et al. 2005). A number of studies have compared the performance of LUR and dispersion modelling (Bell 2006; Briggs et al. 2000; Briggs et al. 1997; Cyrys et al. 2005; Dijkema et al. 2011; Hennig et al. 2016; Jerrett et al. 2005; Marshall et al. 2008; Wu et al. 2011). These studies suggest that LUR models can explain the small-scale variations in air pollution concentrations as well or even better than most dispersion models. Results, however, depend on the characteristics of the study area, the density of the monitoring, and the resolution of the predictor variables. Beelen et al. (2010) compared the performance of high-resolution LUR and dispersion models in estimating small-scale variations in NO<sub>2</sub> concentrations and observed a moderate agreement between the estimated concentrations based on the two methods. The dispersion model performed better than the LUR model with a correlation of 0.77 versus 0.47 against data from fixed stations. Marshall et al. (2008) used three approaches for estimating within-urban spatio-temporal variability in ambient concentrations: (a) spatial interpolation of monitoring data (nearest and inverse distance weighted (IDW)), (b) LUR, and (c) a

Eulerian grid model (CMAQ). The authors found that LUR exhibited higher spatial variability compared to the other methods. Correlations with data from fixed monitoring stations were 76% and 71% for LUR and CMAQ, respectively. Wu et al. (2011) compared different exposure assessment methods in an adverse pregnancy outcome study in Los Angeles and Orange County. Exposures were estimated at residential addresses using (a) the nearest ambient monitoring station, (b) LUR models, (c) a line source dispersion model (CALINE4), and (d) a simple traffic-density measure. The effect estimates were smaller for exposures based on simpler traffic density measures and larger for LUR. More recently, Hennig et al. (2016) compared a dispersion model and a LUR model in Germany noting that the agreement between the two models improved considerably after restricting the dispersion model to local traffic only. Few other studies also compared the use of LUR and dispersion models for exposure assessment. Hoogh et al. (2014) estimated NO<sub>2</sub> exposures at residential locations and found that the dispersion model predicted a moderate to large proportion of the measured variation in NO<sub>2</sub> compared to the LUR model. Gulliver et al. (2011) however found that the LUR model performed significantly better than the dispersion model suggesting that LUR techniques provide robust methods for long-term exposure assessment in epidemiology.

This paper compares four different NO<sub>2</sub> exposure surfaces developed for the City of Montreal. Two of the surfaces are based on LUR models, one was developed using data from passive samplers (Crouse et al. 2009) and another was developed using data from micro-sensors and short-term monitoring (Deville Cavellin et al. 2016). The other two surfaces were both developed based on dispersion modelling; one surface was developed using a regional Gaussian puff dispersion model which can handle terrain effects and incorporates spatially refined meteorology (Shekarzifard et al. 2017), while the other is a street canyon dispersion model which resolves near-road concentrations and flow at road intersections (Fallah-Shorshani et al. 2017). Exposures for participants in breast cancer (BC) and prostate cancer (PC) case-control studies were then derived in order to compare ORs from the four exposure measures.

## 2. Materials and methods

### 2.1. Development of exposure surfaces

#### 2.1.1. Exposure surfaces based on dispersion models

Two different models were adopted in order to disperse traffic emissions in Montreal (Fig. 1). Both models used emissions of nitrogen oxides (NO<sub>x</sub>) estimated at the level of individual road segments and varying by time of day (Sider et al., 2013). In order to generate estimates of on-road emissions, we used data from an origin-destination (OD) trip diary survey conducted during the fall of 2008 (a single day in October) for the Montreal metropolitan area. The 2008 OD data includes information for 5% of the Montreal population with 66,000 households, 157,000 individuals, and 355,000 daily trips (Agence Metropolitaine De Transport (AMT) (2008)). To estimate traffic volumes, driving trips (expanded up to the total population) were assigned on the road network using the PTV VISUM platform (Vision 2009; DMTI, 2010). In addition, vehicle mix and average speed on every local and major road (127,217 road segments) were expressed. The model employs the stochastic user equilibrium approach (SUE) to assign trips onto the network. Using output of the transportation model, we estimated emissions of nitrogen oxides (NO<sub>x</sub>) with the Mobile Vehicle Emissions Simulator (MOVES) platform developed by the United States Environmental Protection Agency (USEPA) updated with Montreal-

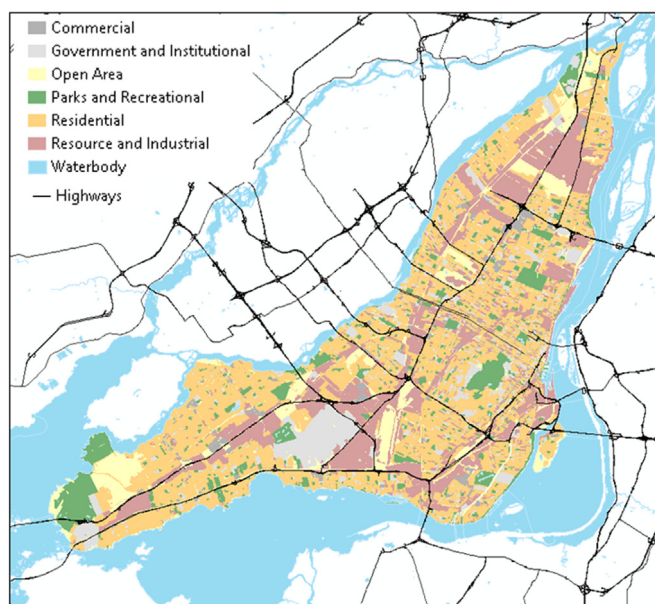


Fig. 1. Montreal Island land-use and highways.

specific data. Using information on vehicle type, model year, speed, road type, and season (winter and summer), individual emission factors were generated. Fuel composition and ambient conditions within MOVES were replaced with Montreal-specific data. We generated fleet-wide emission factors (EFs) for NO<sub>x</sub> in g/veh km, varying by vehicle type (passenger car and passenger truck), age (30 model years), fuel (gasoline and diesel), road type (highway, arterial), and average speed (15 speed bins ranging from 2.5 mph to > 65 mph). Finally, emissions of NO<sub>x</sub> were estimated at the level of every individual vehicle based on its type, age, speed, and type of road. Total emissions on every road segment were computed by summing the individual emissions of all vehicles on that segment.

Hourly emissions for each road were used as input within two different dispersion algorithms in order to simulate hourly NO<sub>2</sub> concentrations. The first dispersion model is a Gaussian model, based on the Lagrangian puff equation, which estimates the growth diffusion and transport of released puffs in the modelling domain. The CALMET-CALPUFF modelling system was used to simulate three-dimensional meteorology and NO<sub>x</sub> dispersion. We used the meteorological model CALMET to interpolate winds and temperatures using higher-resolution terrain elevation, land-use, the fifth-generation NCAR/Penn State Mesoscale Model (MM5), as well as data from 10 surface stations. After generating the three-dimensional meteorology at a resolution of 1 × 1 km, we used the dispersion model CALPUFF which shares the same modelling domain as CALMET. The domain extends 200 km × 140 km (1 km × 1 km grids) centered on the Montreal Island (Shekarzifard et al. 2017). The RIVAD chemical transformation scheme was applied to transfer NO<sub>x</sub> to NO<sub>2</sub>. We used O<sub>3</sub> concentrations as input to the model chemistry in order to transfer NO<sub>x</sub> to nitrate (NO<sub>3</sub>) and nitric acid (HNO<sub>3</sub>). Furthermore, since part of NO<sub>x</sub> that transfers to smog in the presence of hydrocarbons varies with the NO<sub>2</sub>/NO<sub>x</sub> ratio, a nonlinear regression equation between NO<sub>2</sub>/NO<sub>x</sub> ratio and NO<sub>x</sub> was used as input to the chemistry module. The 127,217 roads in Greater Montreal were broken into smaller segments (less than 0.5 km) to increase the accuracy of road source modelling. A value of 3.5 m was considered for the initial vertical dispersion coefficient (sigma z), therefore representing traffic-induced mixing near the roadway. Hourly background NO<sub>2</sub> concentrations were included, using data observed at the city of Montreal's monitoring station number 99, located at the west tip of the Montreal Island. A detailed description of dispersion modelling is provided in Shekarzifard et al. (2017).

A street-canyon model (SIRANE), which is better suited at characterizing air pollution within the urban canopy, was also used. The SIRANE model (Soulhac et al. 2011) is capable of simulating each street with a box model and calculates the corresponding advective fluxes balance at intersections. The street-canyon model SIRANE was used to calculate ambient NO<sub>2</sub> concentrations using the emissions of NO and NO<sub>2</sub> derived from the traffic and emission models. SIRANE is an operational urban dispersion model that adopts parametric relations for the pollutant transfer phenomena within and out of the urban canopy. This model provides the spatial and temporal evolution of concentrations for different pollutants, appropriate to the scale of a neighbourhood or a city (from few hundred meters to about ten km). SIRANE accounts for three important transport mechanisms within the urban canopy to better estimate the effect of the complex street configuration in an urban area including; a) advective mass transfer along the street due to the average wind along its axis, b) turbulent mass transfer across the interface between the street and the overlying atmospheric boundary layer, and c) advective transport at street intersections. Finally, it uses a Gaussian plume model to transport and disperse air pollution above roof level and complete the simulation at street level. SIRANE assumes hourly meteorological data to be uniform across the modelling domain in contrast to the sophisticated meteorological component of CALPUFF. The meteorological data calculated for CALPUFF, were exported and used in the SIRANE model. Resolution of the SIRANE model is the same as CALPUFF (1 × 1 km).

Throughout the remainder of the paper, we refer to the NO<sub>2</sub> surface based on CALPUFF as Dispersion-1 while the surface based on SIRANE is referred to as Dispersion-2.

### 2.1.2. Exposure surfaces based on LUR

We used two NO<sub>2</sub> exposure surfaces for Montreal generated using LUR, developed by Crouse et al. (2009) (referred to as LUR-1) and Deville Cavellin et al. (2016) (referred to as LUR-2).

Briefly, Crouse et al. (2009) conducted a series of two-week sampling campaigns in 2005–2006 to estimate NO<sub>2</sub> concentrations at individual points throughout Montreal. Concentrations of NO<sub>2</sub> were measured at a height of 2.5 m near the sidewalk at 133 locations using two-sided Ogawa passive samplers (Ogawa and Co., USA) during three periods: i) November/December 2005, ii) April/May 2006 and iii) August 2006. A set of variables describing specific land-use and road density characteristics measured at different radial distances away from the samplers were generated (100, 300, 500 and 700 m). With these variables, a LUR model was developed to predict the concentrations of NO<sub>2</sub> where measurements were not taken (the model explained approximately 80% of the variability in measured NO<sub>2</sub> concentrations). The variables computed in LUR-1 model include land-use classification (commercial, governmental/institutional, open areas, parks/recreational, residential, resource/industrial and water body) and building footprint. In addition, population density, number of NPRI (National Pollutant Release Inventory) locations emitting NO<sub>x</sub>, traffic counts, distance to the shoreline, to the nearest highway, and to known point sources of NO<sub>2</sub> (namely the 33 NPRI facilities) were considered. The output of this model is a 5 × 5 m raster-based NO<sub>2</sub> map.

More recently, another LUR surface for NO<sub>2</sub> was developed by Deville Cavellin et al. (2016). In this study, two data collection campaigns were conducted: one spanning 10 weeks (between May and July of 2014) with 76 sites (visited three to eight times) and another spanning 4 weeks in October of 2014 with 35 sites (visited four times each). The sites were visited randomly to have an equal number of rush-hour and off-peak visits for each site. The sites were selected based on a population-weighted location-allocation algorithm meant to represent high spatial variability in traffic intensity and in population density. Aeroqual S500 sensors were used for this campaign. A LUR model was developed which explained approximately 86% of the variability in measured NO<sub>2</sub> concentrations. The land-use variables included: number of bus stops and length of bus routes, number of intersections, number of NPRI locations emitting NO<sub>x</sub> and volatile organic compounds, length of highways, length of major roads, total length of roads, distance to



roads, traffic on the roads, total population, area occupied by different land-use types (commercial, governmental/institutional, open areas, parks/recreational, residential, resource/industrial and water body), and building footprint. Additionally, distances between the sites and potential sources of air pollution, major roads, highways, Montreal International Airport, port of Montreal, shore, nearest rail line, and nearest NPRI locations were considered. The output of this model is a  $100 \times 100\text{m}$  raster-based  $\text{NO}_2$  map.

## 2.2. Comparison of exposure surfaces

Before comparing the surfaces, we validated each surface with data obtained from 9 reference monitoring stations in the city of Montreal. In addition, we compared the observed  $\text{NO}_2$  concentrations at fixed monitoring stations between the years 2006, 2008 and 2014 to capture the temporal variations among these years and to explain whether the differences among the surfaces could be due to changes in  $\text{NO}_2$  concentrations over time.

While both LUR models were generated to represent a mean annual  $\text{NO}_2$  surface, dispersion models have the capability of generating a surface for different times of day (e.g., hourly). For comparative purposes, daily average concentrations based on dispersion models were aggregated.

In order to compare the exposure surfaces generated using dispersion modelling against the Crouse et al. (2009) (LUR-1) and Deville Cavellin et al. (2016) (LUR-2) surfaces, the island of Montreal was subdivided into a mesh and the four  $\text{NO}_2$  values (Dispersion-1, Dispersion-2, LUR-1, LUR-2) were allocated to gridcells of  $1 \times 1\text{km}$  each. Pearson and Spearman correlations as well as scatter plots were developed between pairs of surfaces. In addition, Bland-Altman plots were developed to assess the magnitude of disagreement (including systematic differences) as well as identify outliers. Bland-Altman plots illustrate differences between predictions of two methods against their average (Bland and Altman, 1986). We also examined similarities between pairs of  $\text{NO}_2$  surfaces using the intra-class correlation coefficient (ICC), generated for each forward sorting area (FSA), which indicates the first 3 digits of the postal code. The ICC is a common metric for assessing agreement or consistency between two methods of measurement which share the same observational units of sampling and/or measurement process. We made use of a two-way mixed-effect variance model to derive pairwise ICC with 95% confidence interval.

## 2.3. Analysis of breast and prostate cancer case-control studies

Residences of 792 and 1,772 participants in the breast cancer (BC) and prostate cancer (PC) case-control studies were linked to the four  $\text{NO}_2$  surfaces at the same resolution of 1 km, using ArcGIS 10.4.1. We used BC and PC data from two case-control studies conducted in Montreal, Quebec. A total of 377 BC incident cases were identified between 2008 and 2011 from all but one hospital that treated breast cancer in the Montreal area. (Goldberg et al. 2017). Women were eligible if they fulfilled criteria for being menopausal (i.e., the WHO criteria for menopausal status, accounting for hormone replacement therapy, hysterectomy, and bilateral oophorectomy), were between 50 and 70 years of age, lived on the Island of Montreal, had never had a previous occurrence of any type of cancer, and were registered with the universal Provincial Electoral List. Population controls (415 individuals) were identified randomly from provincial electoral lists of Montreal residents and frequency-matched to cases using 5-year age groups. In the second study, a population-based case-control study of incident prostate cancer during the years 2005–2009 was conducted (Parent et al. 2013; Blanc-Lapierre et al. 2015; Weichenthal et al. 2017). Men less than 76 years of age at the time of prostate cancer diagnosis were selected from the main francophone hospitals that diagnose prostate cancer (802 cases). 968 control subjects were randomly selected from the same districts as the case subjects and frequency-matched to cases in 5-year age groups. Control subjects were still eligible if they had a history of cancer other than prostate cancer. In both studies, exposure to  $\text{NO}_2$  was associated with increased risks of BC and PC after adjusting for other risk factors.

In the present study, we adopted the same methodology and covariates as the original studies to estimate the ORs for both cancers using estimates of  $\text{NO}_2$  exposure. For this purpose, an unconditional logistic regression model was used to estimate ORs and associated 95% confidence intervals (CI). Each exposure measure was included as a continuous linear variable, after verifying this assumption through the use of natural cubic functions of the exposure-response curves. Different sets of covariates were included in the two different cancer studies, and these variables included the cancer-specific set of accepted and suspected risk factors, including age at diagnosis, first degree family history, education, family income, ethnicity, drinking and smoking status, body mass index, and immigration status. Additional risk factors for BC included age at oophorectomy, age at menarche, oral contraception use, duration of hormone replacement therapy use, total duration of breastfeeding, and age at first full-term pregnancy. All risk factors including the number of cancer cases and controls are presented as supplementary material. We included the covariates in the analysis in both forms of linear and natural cubic spline functions. We present ORs for an increase across different interquartile ranges (IQR) of  $\text{NO}_2$  for the four surfaces. The IQR is defined based on the exposures of subjects (combination of cases and controls).

## 3. Results

### 3.1. Comparison of exposure surfaces

The predictions of the four surfaces were compared against  $\text{NO}_2$  data collected at a total of 9 fixed-site air quality monitoring stations managed and operated by the City of Montreal through the Réseau de Surveillance de la Qualité de l'Air (RSQA). Using the predicted-observed pairs at each of the 9 stations, we computed the Pearson and Spearman correlation coefficients for each surface. The Pearson correlations between the observed and predicted values were 0.61 for Dispersion-1; 0.55 for Dispersion-2, 0.87 for LUR-

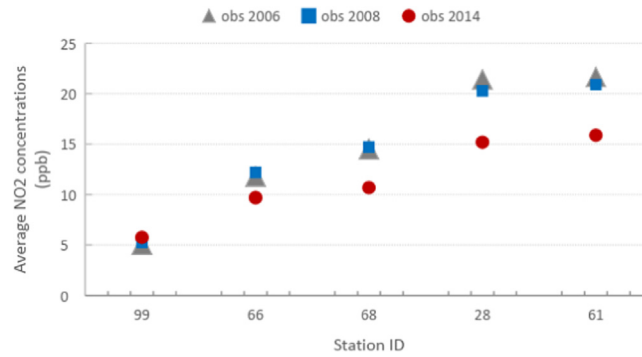


Fig. 2. Trend in NO<sub>2</sub> concentrations at various reference stations in Montreal between 2006 and 2014.

1 and 0.88 for LUR-2. The Spearman correlations were 0.78 for Dispersion-1; 0.67 for Dispersion-2, 0.92 for LUR-1 and 0.86 for LUR-2. In addition, we plotted the average yearly NO<sub>2</sub> concentrations at different monitoring stations across the City of Montreal (Fig. 2). At station 99 which is the background station, the NO<sub>2</sub> concentration trend remained unchanged; the NO<sub>2</sub> concentrations for 2006 and 2008 are similar and higher than 2014 levels at different fixed stations.

Figs. 3a, 3b, 3c and 3d present Dispersion-1, Dispersion-2, LUR-1 and LUR-2 surfaces, in this order, after converting all surfaces to a  $1 \times 1$  Km resolution. Generally, the four surfaces pick-up on the higher concentrations occurring along main highways and closer to the city center as well as the lower concentrations on the western tip of the island, located upwind of the prevailing winds. The Dispersion-1 method (regional Gaussian puff dispersion model) tended to generate lower NO<sub>2</sub> concentrations as compared to the other methods; this is due to 1) the fact that the dispersion model only takes into account the contribution of traffic, and 2) the limited capability of a Gaussian dispersion model to take into account the “trapping” effects of buildings along urban streets. The NO<sub>2</sub> concentrations generated using Dispersion-2 (a street canyon model which resolves the recirculation effect in urban canyons) are closer to LUR-1 and lower than LUR-2 values. LUR-2 (generated using micro-sensors) yielded the highest values. In fact, Deville Cavellin et al. (2016) pointed out sensor oversensitivity when developing LUR-2.

The scatter plots in Fig. 4 illustrate a high agreement between the two dispersion surfaces and especially between the LUR surface

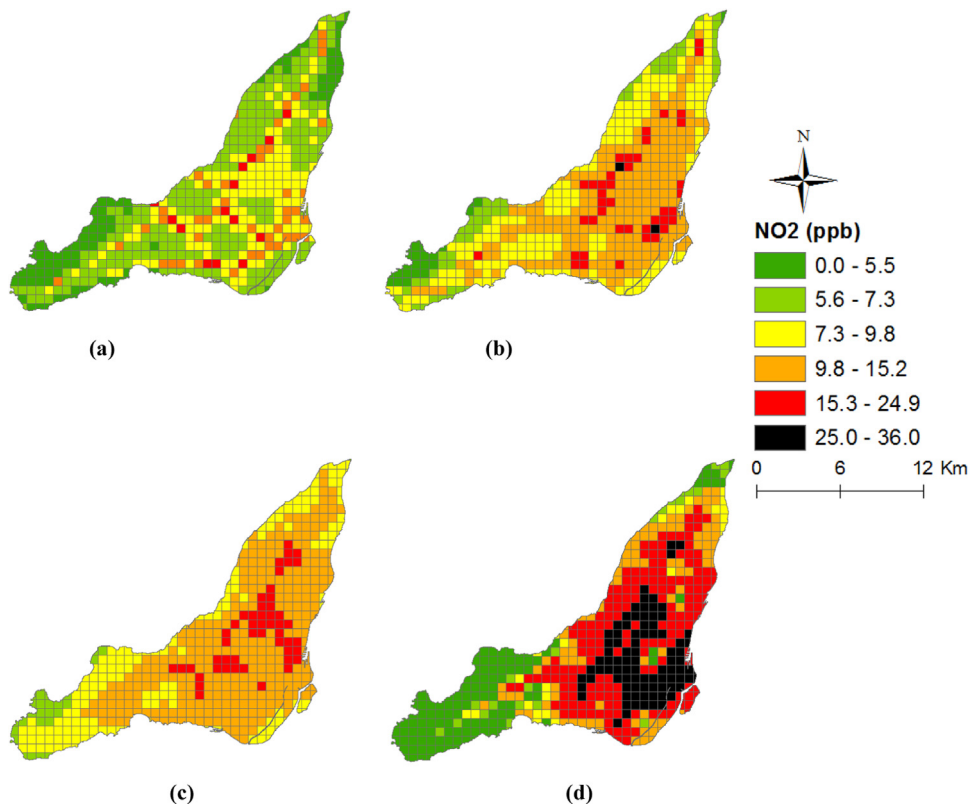
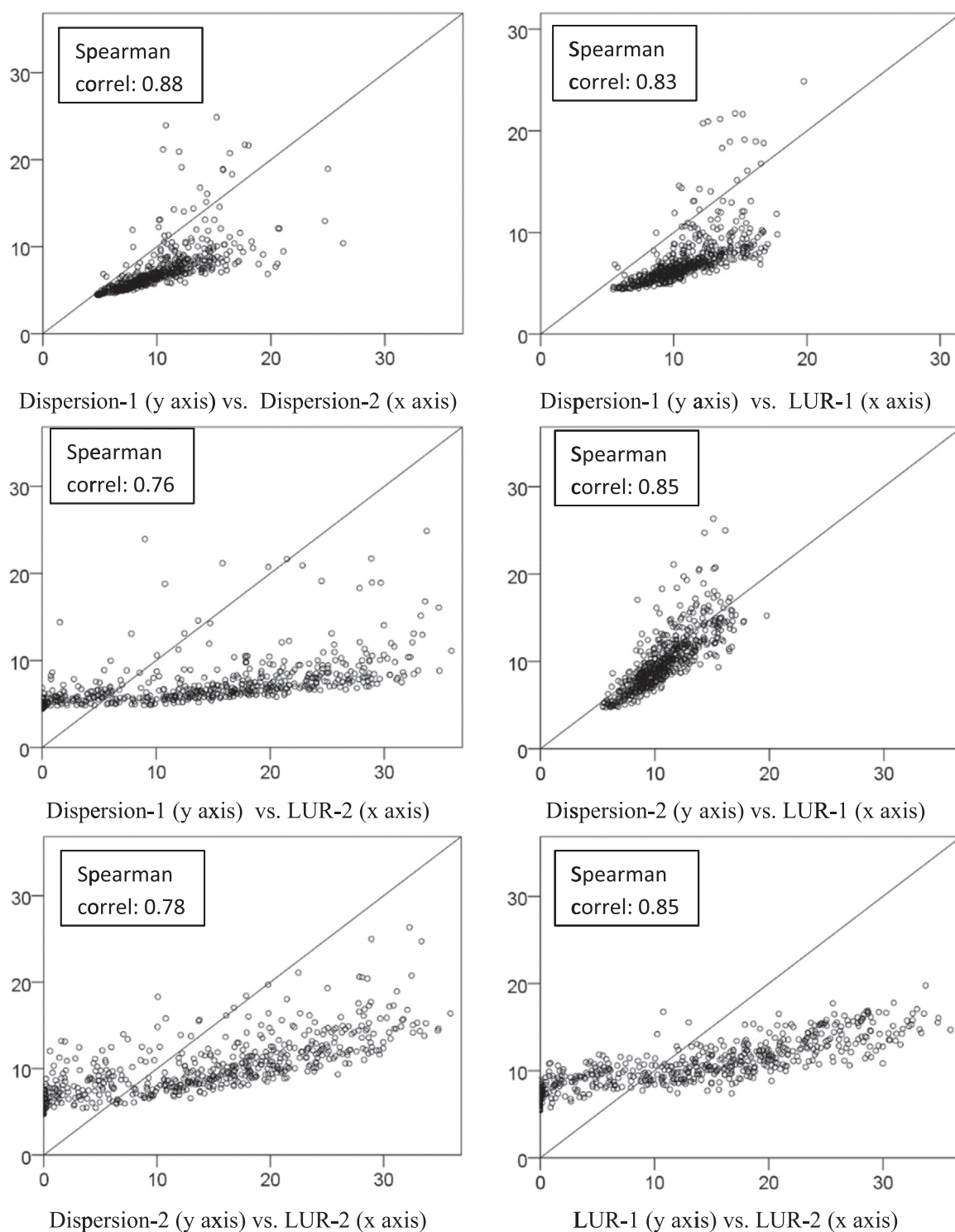


Fig. 3. Visualization of four NO<sub>2</sub> surfaces, Dispersion-1 (a), Dispersion-2 (b), LUR-1 (c), LUR-2 (d).



**Fig. 4.** Scatter plots illustrating the correlation between the exposure surfaces based on dispersion and LUR models.

developed using passive samplers (LUR-1) and the dispersion surface developed using the street canyon model (Dispersion-2). The highest Spearman correlation with data from  $1 \times 1$  Km gridcells is 0.88 between the two dispersion surfaces followed by 0.85 between LUR-1 and LUR-2 as well as between LUR-1 and Dispersion-2 (developed using the street canyon model). The lowest correlation is 0.76 between Dispersion-1 and LUR-2.

Fig. 5 presents the Bland-Altman plots, representing the differences between pairs of surfaces as a function of the mean value of

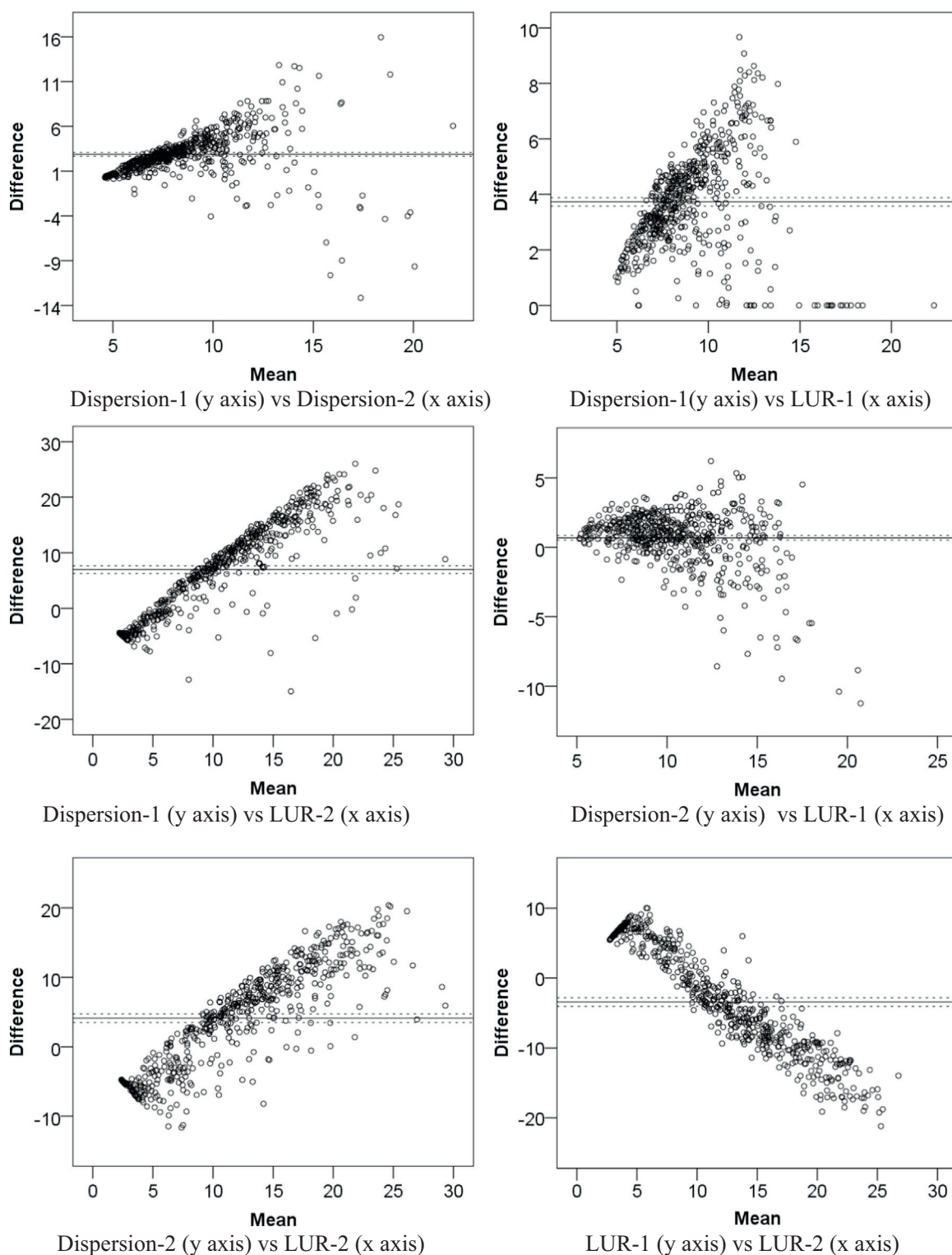
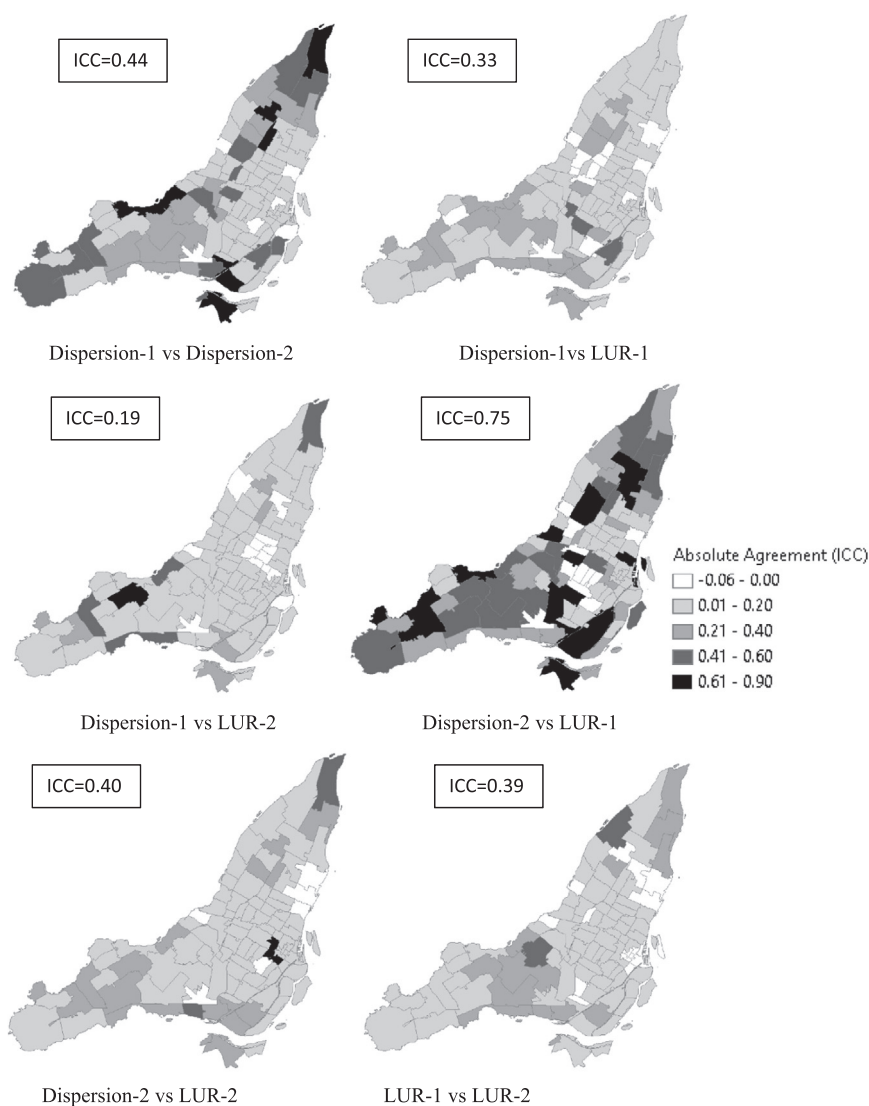


Fig. 5. Bland-Altman plots; the solid line indicates bias and limits of agreement with 95% Confidence Intervals (CI) indicated by the dashed lines.

two surfaces. The solid line represents the mean difference while the limits of agreement (mean  $\pm$  st. dev.) are represented in dotted lines. The 95% limits of agreement (LOA) between the two dispersion models and between Dispersion-2 and LUR-1 are narrower compared to other pairs of surfaces. This analysis highlights again the agreement between the dispersion model based on passive





**Fig. 6.** Maps of pairwise NO<sub>2</sub> absolute agreement ICC by Forward Sorting Area (FSA). A higher ICC (black and dark grey) is noted between the Dispersion-2 and LUR-1 methods followed by Dispersion-1 and Dispersion-2. The lowest ICC (white and light gray) was estimated between Dispersion-1 and LUR-2. The ICCs in the top left corner of each map show the average ICC for all FSAs.

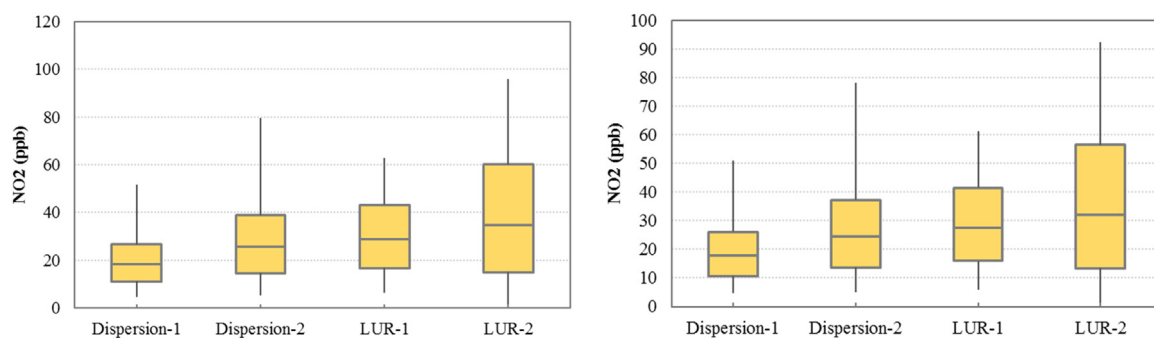


**Fig. 7.** Distribution of exposures for breast cancer (left) and prostate cancer (right) subjects based on the four surfaces.

**Table 1**

Spearman correlations of exposures for breast (a) and prostate (b) cancer subjects.

	Dispersion-1 Gaussian model	Dispersion-2 Street canyon model	LUR-1 Passive samplers	LUR-2 Micro- sensors
(a) Breast cancer (BC)				
Dispersion-1	1	0.78**	0.88**	0.70**
Dispersion-2		1	0.79**	0.70**
LUR-1			1	0.78**
LUR-2				1
(b) Prostate cancer (PC)				
Dispersion-1	1.00	0.79**	0.85**	0.77**
Dispersion-2		1.00	0.78**	0.74**
LUR-1			1.00	0.84**
LUR-2				1.00

\*\* Correlation is significant at the 0.01 level (2-tailed)

samplers (LUR-1) and the street canyon model (Dispersion-2).

Finally, Fig. 6 presents the pairwise, ICC developed at the level of FSAs (first 3-digit of postal code). A higher ICC is noted between the Dispersion-2 and LUR-1 methods followed by Dispersion-1 and Dispersion-2, where 13.5% and 6% of FSA zones have ICC > 0.60. The lowest disagreement was found between Dispersion-1 (Gaussian model) and LUR-2 (based on micro-sensors) where 88 of the 96 FSAs have an ICC of 0.20 and lower (A high ICC close to 1 indicates high similarity between values from the same group. A low ICC close to zero means that values from the same group are dissimilar).

### 3.2. Analysis of exposure for subjects in BC and PC case-control studies

Fig. 7 shows the distribution of NO<sub>2</sub> exposures for BC and PC subjects, respectively. There is a higher variability and range of exposures based on the LUR models, compared with the dispersion models. As expected, exposures are highest based on LUR-2 (micro-sensors) and relatively similar for LUR-1 (passive samplers) and Dispersion-2 (street canyon model). Pairwise correlations (Spearman) between exposures derived from the different surfaces were generally similar to the correlations between the surfaces at the level of gridcells (Table 1).

### 3.3. Estimates of risk for breast and prostate cancer

The fully-adjusted ORs for BC and PC for an increase in the IQR based on exposures derived from the four surfaces are presented in Table 2. For BC, the lowest estimate of risk is 1.05 and the highest is 1.26. For PC, the lowest OR is equal to 1.04, and the highest 1.39. These estimates indicate that despite the range in possible exposures, the association between exposure and the risk of BC or PC is likely to be positive. For both BC and PC, the ORs based on the dispersion surfaces are lower than the ORs based on LUR surfaces. We observed higher mean ORs based on the LUR surfaces but with overlapping CIs. Since LUR models capture all sources of NO<sub>2</sub> and dispersion models only capture traffic emissions, it is possible that this difference is due to the fact that non-road sources also contribute to the spatial distribution in NO<sub>2</sub> concentrations. Performance of the logistic regression for fully adjusted models are presented in detail in the supplementary materials.

**Table 2**Fully-adjusted ORs for postmenopausal breast cancer and prostate cancer derived for an increase equal to each interquartile range from four surfaces of NO<sub>2</sub>.

Surface	BC		PC	
	OR	95% CI	OR	95% CI
Dispersion-1 Gaussian model	1.07	0.94, 1.23	1.13	1.03, 1.24
Dispersion-2 Street canyon model	1.05	0.90, 1.22	1.04	0.94, 1.16
LUR-1 Passive samplers	1.26	0.97, 1.63	1.39	1.14, 1.69
LUR-2 Micro-sensors	1.10	0.89, 1.37	1.30	1.08, 1.56

\*The IQR for breast cancer is 3.694 ppb for LUR-1, 2.084 ppb for Dispersion-1, 10.188 ppb for LUR-2, and 3.915 ppb for Dispersion-2. The IQR for prostate cancer is 3.85 ppb for LUR-1, 2.17 ppb for Dispersion-1, 10.93 ppb for LUR-2, and 4.36 ppb for Dispersion-2.

#### 4. Discussion

The analysis we presented in this study sheds light on the use of four different measures of exposure to traffic-related air pollution. Our main objective was to compare the distribution of the spatial estimates of NO<sub>2</sub> computed from two dispersion models to the distribution of NO<sub>2</sub> obtained from two LUR models. A secondary objective was to compare estimates of risk using these four exposure estimates; in doing so, we exploited two case-control studies of cancer conducted previously. The main advantage of using air quality models to derive exposure relates to their policy sensitivity, one could potentially evaluate the effects of changes in land-use, transportation infrastructure, and travel demand on traffic emissions and re-investigate the same associations with health outcomes.

We estimated separate ORs using concentrations of NO<sub>2</sub> using the four surfaces as measures of exposure, both for the BC and PC case-control studies. In total, 792 individuals were included in the BC study and 1722 subjects were included in the PC study (including both cases and controls). Results show that the risk estimates using the two LUR exposure surfaces were between 10–26% for BC and 30–39% for PC which were higher than the risk estimates generated by the dispersion surfaces (5–7% for BC and 4–13% for PC).

To the extent to which dispersion models incorporate robust algorithms able to capture the temporal and spatial variability in NO<sub>2</sub> concentrations, our surfaces do not include estimates of truck emissions and industrial sources, leading to lower concentrations compared to the LUR surfaces. As a result, part of the differences in ORs between the dispersion and LUR models are due to the lack of these emission sources in dispersion modelling. The differences between the two dispersion surfaces are mostly attributable to the nature of the two models and chemical transformation processes. We also note systematic differences in measurements between passive samplers and low-cost sensors. Areas with lower ICCs and higher disagreement between each pair of surfaces were mostly located near the downtown and denser areas. The areas of higher agreement were most likely affected by lower emissions from traffic, and are located west of the island which includes typical suburban developments with lower building and population density than the inner city core. It is also important to note that we compared two dispersion surfaces obtained from 2008 traffic data against two LUR surfaces based on 2006 and 2013 monitoring campaigns.

The present study fills a gap in the existing literature by comparing the methods that are often used to derive air pollution exposure in epidemiological studies (Bell 2006; Hennig et al. 2016). Various studies compared spatial interpolation methods (e.g., kriging, IDW and nearest monitor) with LUR techniques (Brauer et al. 2008) and only few of them compared spatial interpolation methods with atmospheric dispersion models (Bell 2006; Hennig et al. 2016; Wu et al. 2011). In addition, this study illustrates the effects of using each of the four different measures of exposure on the increased risk of two cancers, previously associated with exposure to traffic related air pollution.

Application of these different approaches leads to differences in exposure estimation and interpretation due to the specific characteristics of each method. Bell (2006) found that air quality modelling systems may be able to provide better estimates of exposure than monitoring alone. Wu et al. (2011) compared effect estimates for traffic-related air pollution exposure surfaces and preterm birth using monitoring stations, LUR and dispersion surfaces in Los Angeles and Orange County. They observed that the size of effect estimates was smaller for exposures based on measurements compared to more refined exposure assessment methods. Similar to our study, Henning et al. (2016) found that the agreement between a chemical transport model and a LUR model was weak to moderate and that LUR models estimate more stable long-term exposures to local, mostly traffic-related air pollution with respect to very small-scale spatial variations.

In this study, the four modelling approaches were found to reflect slightly different spatial variations in NO<sub>2</sub> concentrations, however the surfaces based on the two dispersion models and LUR models were highly correlated. Additionally, for all four surfaces, we found a positive association with the increase in NO<sub>2</sub> concentrations and risk of breast and prostate cancers, but we observed higher ORs using the LUR exposure surfaces.

The higher ORs associated with the LUR surfaces indicate that the surfaces based on the dispersion models have led to potential misclassification in the exposure estimates, thus leading to lower estimates of risk. Indeed, by examining the distributions of exposures associated with the home locations of participants based on the four surfaces, we observe that the range and variability in exposures is higher with LUR models than dispersion models. This is an indication that the LUR models are able to better capture the intra-urban variability in NO<sub>2</sub> concentrations and to better express the range of exposures in an urban area.

#### Information on funding sources supporting the work

This study was funded by a collaborative grant from the Canadian Institutes of Health Research and the Natural Sciences and Engineering Research Council of Canada through the Collaborative Health Research Projects (2015–2018). Special thanks are extended to Joseph Scire, David Strimaitis and the entire CALPUFF development team for their immense assistance throughout this study. Special thanks are extended to Lionel Soulhac, Perrine Charvolin-Volta, and the SIRANE development team. Thanks to Sophie Goudreau for providing the building height data as well as for granting technical support in PostGIS. The cancer study was supported financially through grants from the Canadian Cancer Society (grants no. 13149, 19500, 19864, 19865), the Cancer Research Society, the Fonds de Recherche du Québec - Santé (FRQS), FRQS-RRSE, and the Ministère du Développement économique, de l'Innovation et de l'Exportation du Québec.

#### Conflict of interest

The authors report that they have no conflicts of interest.

## References

- Abernethy, R.C., Allen, R.W., Mckendry, I.G., Brauer, M., 2013. A land use regression model for ultrafine particles in Vancouver, Canada. *Environ. Sci. Technol.* 47, 5217–5225.
- Agence Metropolitaine De Transport (AMT), 2008. La mobilité des personnes dans la région de Montréal: faits saillants. Enquête Orig.-Destin.
- Andersen, Z.J., Hvidberg, M., Jensen, S.S., Ketzel, M., Loft, S., Sørensen, M., et al., 2011. Chronic obstructive pulmonary disease and long-term exposure to traffic-related air pollution. *Am. J. Resp. Crit. Care Med.* 183 (4), 455–461.
- Austin, C.C., Roberge, B., Goyer, N., 2006. Cross-sensitivities of electrochemical detectors used to monitor worker exposures to airborne contaminants: false positive responses in the absence of target analytes. *J. Environ. Monit.* 8, 161–166.
- Batterman, S.A., Zhang, K., Kononowech, R., 2010. Prediction and analysis of near-road concentrations using a reduced-form emission/dispersion model. *Environ. Health* 9 (29–29).
- Beckx, C., Panis, L.I., Uljee, I., Arentze, T., Janssens, D., Wets, G., 2009. Disaggregation of nation-wide dynamic population exposure estimates in the Netherlands: applications of activity-based transport models. *Atmos. Environ.* 43, 5454–5462.
- Beelen, R., Hoek, G., Vienneau, D., Eeftens, M., Dimakopoulou, K., Pedeli, X., Tsai, M.-Y., Künzli, N., Schikowski, T., Marcon, A., Eriksen, K.T., Raaschou-Nielsen, O., Stephanou, E., Patelarou, E., Lanki, T., Yli-Tuomi, T., Declercq, C., Falq, G., Stempfelet, M., Birk, M., Cyrys, J., Von Klot, S., Nádor, G., Varró, M.J., Dèdelé, A., Gražulevičienė, R., Mölter, A., Lindley, S., Madsen, C., Cesaroni, G., Ranzi, A., Badaloni, C., Hoffmann, B., Nonnemacher, M., Krämer, U., Kuhlbusch, T., Cirach, M., De Nazelle, A., Nieuwenhuijsen, M., Bellander, T., Korek, M., Olsson, D., Strömberg, M., Dons, E., Jerrett, M., Fischer, P., Wang, M., Brunekreef, B., De Hoogh, K., 2013. Development of NO<sub>2</sub> and NO<sub>x</sub> land use regression models for estimating air pollution exposure in 36 study areas in Europe – The ESCAPE project. *Atmos. Environ.* 72, 10–23.
- Beelen, R., Voogt, M., Duyzer, J., Zandveld, P., Hoek, G., 2010. Comparison of the performances of land use regression modelling and dispersion modelling in estimating small-scale variations in long-term air pollution concentrations in a Dutch urban area. *Atmos. Environ.* 44, 4614–4621.
- Bell, M.L., 2006. The use of ambient air quality modeling to estimate individual and population exposure for human health research: a case study of ozone in the Northern Georgia Region of the United States. *Environ. Int.* 32, 586–593.
- Bellander, T., Berglind, N., Gustavsson, P., Jonson, T., Nyberg, F., Pershagen, G., Järup, L., 2001. Using geographic information systems to assess individual historical exposure to air pollution from traffic and house heating in Stockholm. *Environ. Health Perspect.* 109, 633.
- Blanc-Lapierre, A., Spence, A., Karakiewicz, P.I., Aprikian, A., Saad, F., Parent, M.E., 2015. Metabolic syndrome and prostate cancer risk in a population-based case-control study in Montreal, Canada. *BMC Public Health* 15 (2015), 913.
- Bland, J.M., Altman, D., 1986. Statistical methods for assessing agreement between two methods of clinical measurement. *Lancet* 327, 307–310.
- Brauer, M., Lencar, C., Tamburic, L., Koehoorn, M., Demers, P., Karr, C., 2008. A cohort study of traffic-related air pollution impacts on birth outcomes. *Environ. Health Perspect.* 116, 680.
- Briggs, D.J., Collins, S., Elliott, P., Fischer, P., Kingham, S., Lebre, E., Pryl, K., Van Reeuwijk, H., Smallbone, K., Van Der Veen, A., 1997. Mapping urban air pollution using GIS: a regression-based approach. *Int. J. Geogr. Inf. Sci.* 11, 699–718.
- Briggs, D.J., De Hoogh, C., Gulliver, J., Willis, J., Elliott, P., Kingham, S., Smallbone, K., 2000. A regression-based method for mapping traffic-related air pollution: application and testing in four contrasting urban environments. *Sci. Total Environ.* 253, 151–167.
- Carlsten, C., Dybuncio, A., Becker, A., Chan-Yeung, M., Brauer, M., 2010. Traffic-related air pollution and incident asthma in a high-risk birth cohort. *Occup. Environ. Med.* 2010, 055152.
- Chen, H., Goldberg, M.S., Burnett, R.T., Jerrett, M., Wheeler, A.J., Villeneuve, P.J., 2013. Long-term exposure to traffic-related air pollution and cardiovascular mortality. *Epidemiology* 24, 35–43.
- Cimorelli, A.J., Perry, S.G., Venkatram, A., Weil, J.C., Paine, R.J., Wilson, R.B., Lee, R.F., Peters, W.D., Brode, R.W., 2005. AERMOD: a dispersion model for industrial source applications. Part I: general model formulation and boundary layer characterization. *J. Appl. Meteorol.* 44, 682–693.
- Crouse, D.L., Goldberg, M.S., Ross, N.A., 2009. A prediction-based approach to modelling temporal and spatial variability of traffic-related air pollution in Montreal, Canada. *Atmos. Environ.* 43, 5075–5084.
- Crouse, D.L., Goldberg, M.S., Ross, N.A., Chen, H., Labrèche, F., 2010. Postmenopausal breast cancer is associated with exposure to traffic-related air pollution in Montreal, Canada: a case-control study. *Environ. Health Perspect.* 118, 1578–1583.
- Cyrys, J., Hochadel, M., Gehring, U., Hoek, G., Diekmann, V., Brunekreef, B., Heinrich, J., 2005. GIS-based estimation of exposure to particulate matter and NO<sub>2</sub> in an urban area: stochastic versus dispersion modeling. *Environ. Health Perspect.* 987–992.
- Deville Cavellin, L., Weichenthal, S., Tack, R., Ragettli, M., Smargiassi, A., Hatzopoulou, M., 2016. Investigating the use of portable air pollution sensors to capture the spatial variability of traffic related air pollution. *Environ. Sci. Technol.* 50 (1), 313–320.
- Dijkema, M.B., Gehring, U., van Strien, R.T., et al., 2011. A comparison of different approaches to estimate small-scale spatial variation in outdoor NO<sub>2</sub> concentrations. *Environ. Health Perspect.* 119 (5), 670–675. <https://doi.org/10.1289/ehp.0901818>.
- DMTI, 2010. DMTI Spatial Inc., Database 2007. CanMap Street files.
- Dons, E., Van Poppel, M., Int Panis, L., De Prins, S., Berghmans, P., Koppen, G., Matheeußen, C., 2014. Land use regression models as a tool for short, medium and long term exposure to traffic related air pollution. *Sci. Total Environ.* 476, 378–386.
- Eichhorn, J., Kniffka, A., 2010. The numerical flow model MISKAM: state of development and evaluation of the basic version. *Meteorol. Z.* 19, 81–90.
- Fallah-Shorshani, M., Shekarrizfard, M., Hatzopoulou, M., 2017. Integrating a street-canyon model with a regional Gaussian dispersion model for improved characterisation of near-road air pollution. *Atmos. Environ.*
- Gan, W., Koehoorn, M., Davies, H., Demers, P., Tamburic, L., Brauer, M., 2011. Long-term exposure to traffic-related air pollution and the risk of coronary heart disease hospitalization and mortality. *Epidemiology* 22, S30.
- Gauderman, W.J., Avol, E., Lurmann, F., et al., 2005. Childhood asthma and exposure to traffic and nitrogen dioxide. *Epidemiology* 16 (6), 737–743.
- Gehring, U., Wijga, A.H., Brauer, M., Fischer, P., De Jongste, J.C., Kerkhof, M., Oldenwening, M., Smit, H.A., Brunekreef, B., 2010. Traffic-related air pollution and the development of asthma and allergies during the first 8 years of life. *Am. J. Respir. Crit. Care Med.* 181, 596–603.
- Gulliver, J., Hoogh, K., Fecht, D., Vienneau, D., Briggs, D., 2011. Comparative assessment of GIS-based methods and metrics for estimating long-term exposures to air pollution. *Atmos. Environ.* 45 (39), 7072–7080.
- Hamra, G.B., Laden, F., Cohen, A.J., Raaschou-Nielsen, O., Brauer, M., Loomis, D., 2015. Lung cancer and exposure to nitrogen dioxide and traffic: a systematic review and meta-analysis. *Environ. Health Perspect.*
- Hatzopoulou, M., Miller, E.J., 2010. Linking an activity-based travel demand model with traffic emission and dispersion models: transport's contribution to air pollution in Toronto. *Transp. Res. Part D: Transp. Environ.* 15, 315–325.
- Henderson, S., Brauer, M., MacNab, Y.C., Kennedy, S.M., 2011. Three measures of forest fire smoke exposure and their associations with respiratory and cardiovascular health outcomes in a population-based cohort. *Environ. Health Perspect.* 119 (9), 1266–1271.
- Hennig, F., Sugiri, D., Tzivian, L., Fuks, K., Moebus, S., Jöckel, K.-H., Vienneau, D., Kuhlbusch, T.A., De Hoogh, K., Memmesheimer, M., 2016. Comparison of land-use regression modeling with dispersion and chemistry transport modeling to assign air pollution concentrations within the Ruhr area. *Atmosphere* 7, 48.
- Hertel, O., Berkowicz, R., 1989. Modelling NO<sub>2</sub> concentrations in a street canyon. *DMU Luft A-131*, 31p.
- Hoek, G., Beelen, R., De Hoogh, K., Vienneau, D., Gulliver, J., Fischer, P., Briggs, D., 2008. A review of land-use regression models to assess spatial variation of outdoor air pollution. *Atmos. Environ.* 42, 7561–7578.
- Hoogh, K., et al., 2014. Comparing land use regression and dispersion modelling to assess residential exposure to ambient air pollution for epidemiological studies. *Environ. Int.* 73, 382–392.
- Ihrig, M.M., Shalat, S.L., Baynes, C., 1998. A hospital-based case-control study of stillbirths and environmental exposure to arsenic using an atmospheric dispersion model linked to a geographical information system. *Epidemiology* 9, 290–294.
- Jerrett, M., Arain, A., Kanaroglou, P., Beckerman, B., Potoglou, D., Sahuvaroglu, T., Morrison, J., Giovis, C., 2005. A review and evaluation of intraurban air pollution

- exposure models. *J. Expo. Sci. Environ. Epidemiol.* 15, 185–204.
- Lee, G., You, S., Ritchie, S.G., Saphores, J.-D., Sangkapichai, M., Jayakrishnan, R., 2009. Environmental impacts of a major freight corridor. *Transp. Res. Rec.: J. Transp. Res. Board* 2123, 119–128.
- Lee, J.-H., Wu, C.-F., Hoek, G., De Hoogh, K., Beelen, R., Brunekreef, B., Chan, C.-C., 2014. Land use regression models for estimating individual NO<sub>x</sub> and NO<sub>2</sub> exposures in a metropolis with a high density of traffic roads and population. *Sci. Total Environ.* 472, 1163–1171.
- Levesque, S., Surace, M.J., McDonald, J., Block, M.L., 2011. Air pollution & the brain: subchronic diesel exhaust exposure causes neuroinflammation and elevates early markers of neurodegenerative disease. *J. Neuroinflamm.* 8, 105.
- Levy, J., Clougherty, J., Baxter, L., Houseman, E., Paciorek, C., 2010. Evaluating heterogeneity in indoor and outdoor air pollution using land-use regression and constrained factor analysis. *Res. Report. (Health Eff. Inst.)* 5-80, 81–91 (discussion).
- Marshall, J.D., Nethery, E., Brauer, M., 2008. Within-urban variability in ambient air pollution: comparison of estimation methods. *Atmos. Environ.* 42, 1359–1369.
- McAdam, K., Steer, P., Perrotta, K., 2011. Using continuous sampling to examine the distribution of traffic related air pollution in proximity to a major road. *Atmos. Environ.* 45, 2080–2086.
- Milliez, M., Carissimo, B., 2007. Numerical simulations of pollutant dispersion in an idealized urban area, for different meteorological conditions. *Bound.-Layer Meteorol.* 122, 321–342.
- Nafstad, P., Haheim, L.L., Oftedal, B., Gram, F., Holme, I., Hijermann, I., Leren, P., 2003. Lung cancer and air pollution: a 27 year follow up of 16209 Norwegian men. *Thorax* 58, 1071–1076.
- Ning, Z., Cheung, C.S., Lu, Y., Liu, M.A., Hung, W.T., 2005. Experimental and numerical study of the dispersion of motor vehicle pollutants under idle condition. *Atmos. Environ.* 39, 7880–7893.
- Nyhan, M., McNabola, A., Misstear, B., 2014. Comparison of particulate matter dose and acute heart rate variability response in cyclists, pedestrians, bus and train passengers. *Sci. Total Environ.* 468, 821–831.
- Parent, M.-É., Goldberg, M.S., Crouse, D.L., Ross, N.A., Chen, H., Valois, M.-F., Liautaud, A., 2013. Traffic-related air pollution and prostate cancer risk: a case-control study in Montreal, Canada. *Occup. Environ. Med. (oemed-2012-101211)*.
- Pattinson, W., Longley, I., Kingham, S., 2014. Using mobile monitoring to visualise diurnal variation of traffic pollutants across two near-highway neighbourhoods. *Atmos. Environ.* 94, 782–792.
- Raaschou-Nielsen, O., Bak, H., Sørensen, M., Solvang Jensen, S., Ketzel, M., Hvidberg, M., Schnohr, P., Tjønneland, A., Overvad, K., Loft, S., 2010. Air pollution from traffic and risk for lung cancer in three Danish cohorts. *Cancer Epidemiol. Biomarkers Prev.* 19 (5). <https://doi.org/10.1158/1055-9965.EPI-10-0036>.
- Sangkapichai, M., Saphores, J.-D.M., Ogunseitan, O., Ritchie, S.G., You, S.I., Lee, G., 2010. An Analysis of the Health Impacts from Pm and Nox Emissions Resulting from Train Operations in the Alameda Corridor, CA. University of California Transportation Center, California, USA.
- Scire, J.S., Strimaitis, D.G., Yamartino, R.J., 2000. A user's guide for the CALPUFF dispersion model. *Earth Tech. Inc.* 521. Earth Tech, Inc., pp. 1–521.
- Setton, E., Marshall, J.D., Brauer, M., Lundquist, K.R., Hystad, P., Keller, P., Cloutier-Fisher, D., 2011. The impact of daily mobility on exposure to traffic-related air pollution and health effect estimates. *J. Expo. Sci. Environ. Epidemiol.* 21, 42.
- Shekarrizfard, M., Faghih-Imani, A., Tetreault, L.-F., Yasmin, S., Reynaud, F., Morency, P., Plante, C., Drouin, L., Smargiassi, A., Eluru, N., 2017. Modelling the spatio-temporal distribution of ambient nitrogen dioxide and investigating the effects of public transit policies on population exposure. *Environ. Model. Softw.* 91, 186–198.
- Shekarrizfard, M., Valois, M.-F., Goldberg, M.S., Crouse, D., Ross, N., Parent, M.-E., Yasmin, S., Hatzopoulou, M., 2015. Investigating the role of transportation models in epidemiologic studies of traffic related air pollution and health effects. *Environ. Res.* 140, 282–291.
- Sider, T., Alam, A., Zukari, M., Dugum, H., Goldstein, N., Eluru, N., Hatzopoulou, M., 2013. Land-use and socio-economics as determinants of traffic emissions and individual exposure to air pollution. *J. Transp. Geogr.* 33, 230–239.
- Snowden, J.M., Mortimer, K.M., Dufour, M.-S.K., Tager, I.B., 2014. Population intervention models to estimate ambient NO<sub>2</sub> health effects in children with asthma. *J. Expo. Sci. Environ. Epidemiol.*
- Soulhac, L., Salizzoni, P., Cierco, F.-X., Perkins, R., 2011. The model SIRANE for atmospheric urban pollutant dispersion; part I, presentation of the model. *Atmos. Environ.* 45, 7379–7395.
- Vision, P., 2009. VISUM11.0 Basics. PTV AG, Karlsruhe, Germany.
- Wang, S., Zhang, J., Zeng, X., Zeng, Y., Wang, S., Chen, S., 2009. Association of traffic-related air pollution with children's neurobehavioral functions in Quanzhou, China. *Environ. Health Perspect.* 117, 1612.
- Weichenthal, S., Kulka, R., Dubeau, A., Martin, C., Wang, D., Dales, R., 2011. Traffic-related air pollution and acute changes in heart rate variability and respiratory function in urban cyclists. *Environ. Health Perspect.* 119, 1373–1378.
- Weichenthal, S., Lavigne, E., Valois, M.-F., Hatzopoulou, M., Van Ryswyk, K., Shekarrizfard, M., Villeneuve, P.J., Goldberg, M.S., Parent, M.-E., 2017. Spatial variations in ambient ultrafine particle concentrations and the risk of incident prostate cancer: a case-control study. *Environ. Res.* 156, 374–380.
- Wu, J., Wilhelm, M., Chung, J., Ritz, B., 2011. Comparing exposure assessment methods for traffic-related air pollution in an adverse pregnancy outcome study. *Environ. Res.* 111, 685–692.